Macro-deformed coherent states and the q-analogue quantized field

1997 J. Phys. A: Math. Gen. 30 949

(http://iopscience.iop.org/0305-4470/30/3/019)

J. Phys. A: Math. Gen. **30** (1997) 949–971. Printed in the UK PII: S0305-4470(97)75710-X

Macro-deformed coherent states and the q-analogue quantized field

William C Kimler IV† and Charles A Nelson‡

Department of Physics, State University of New York at Binghamton, Binghamton, NY 13902-6016, USA

Received 24 June 1996

Abstract. The q-analogue coherent states $|z\rangle_q$ are used to identify some of the canonical physical properties of the single-mode of the q-analogue quantized radiation field. Macro-deformed coherent states (CSs) with striking number and phase signatures are found to arise as $q \to \infty$, equivalently as $q \to 0$. In particular, the CS expectation value of the mean number of particles, ${}_q\langle z|N|z\rangle_q \approx \boldsymbol{S}_q(\log_{10}|z|^2)$ where $\boldsymbol{S}_q(\log_{10}|z|^2)$ is a 'stair function' with equally spaced, integer steps as $\log_{10}|z|^2$ increases. Macro q-deformation provides a simple model with one region which simultaneously exhibits features from two distinct regions in the well known bosonic case: the quantum mechanical limit with occupation number $|n\rangle$ states and the semi-classical limit with $|z\rangle$ coherent states where $|z|$ is large. The role of the deformation parameter 'q' is to enable a smooth interpolation between the classic bosonic CSs ($q = 1$) and the fermionic CSs ($q = \infty$ or 0).

1. Introduction

The objectives of this paper are limited. The first is to investigate macro q-deformations, $q \to \infty$ (equivalently $q \to 0$), of the q-analogue coherent states, $a|z\rangle_q = z|z\rangle_q$, and of the associated single-mode of the q-analogue quantized field. The second is to use the simplicity of the behaviours in this region of the coherent state expectation values, ${}_q\langle z|\hat{O}|z\rangle_q$, to investigate general physics issues associated with q-deformation in quantum mechanics and/or in quantum field theory.

The history of the idea of q-bosons is something of a reversal of the well known logic for ordinary bosons (photons, phonons, ...) which correspond to $q = 1$. In 1989, in analogy with Schwinger's oscillator realization of ordinary Lie algebras, MacFarlane and Biedenharn [1, 2] independently introduced a q-oscillator realization, $J_+ = a_1^\dagger a_2, \ldots$, of the new quantum algebras, e.g. of $SU(2)_q$. Recent reviews of quantum algebras and of their applications in mathematical physics include [3]. The q-oscillator commutation relations are

$$a_i a_i^\dagger - q^{\pm 1/2} a_i^\dagger a_i = q^{\mp N_i/2} \qquad i = 1, 2 \tag{1}$$

with $[a_i, a_j^\dagger] = 0$, for $i \neq j, \ldots$ (see below). Following their work, it was then reasoned that if such symmetries were to occur in nature, it would be natural for there also to exist q-bosons and a q-analogue quantum field which has such q-oscillators as its normal modes.

† E-mail address: wkimler@epics.net
‡ E-mail address: cnelson@bingvmb.cc.binghamton.edu

0305-4470/97/030949+23$19.50

So in order to recognize the presence of q-bosons, one needs to know their canonical physical properties. In particular, what are their number and phase signatures? Since quasi-classical coherent states approximately characterize many types of cooperative behaviour in the usual bosonic ($q = 1$) case, One can use the q-analogue coherent states $|z\rangle_q$ to study and identify experimental signatures of a generic single-mode q-analogue quantized field for cooperative phenomena.

Accordingly, in [4] the $|z\rangle_q$ 'classical limit' where $|z|$ is large was studied for fixed q values near to the usual $q = 1$ bosonic region, specifically for $\simeq \frac{1}{16} \leqslant q < 1$. The focus in the present paper is, instead, on the region of macrodeformation: we hold $|z|$ fixed and study the behaviour of CS expectation values, ${}_q\langle z|\hat{O}|z\rangle_q$, as $q \to \infty$ (equivalently as $q \to 0$). In this region, remarkably simple number and phase signatures are found to occur. These are properties of the $|z\rangle_q$ CSs of the system (e.g. of a q-bosonic cooperative phenomenon) and are to be kept mentally distinct from properties exhibited by individual q-bosonic quanta in an occupation number, or Fock, basis.

For an easy overview of what occurs in the case of macro q-deformation, the reader can simply examine the first eight figures and their captions. In the associated text we use the methods of [5] to analytically obtain CS expectation values ${}_q\langle z|\hat{O}|z\rangle_q$ to leading order in q as $q \to 0$. These analytic results agree with the numerical results for $q = 10^{-15}$ which are displayed in the figures. Additional figures for $q = 10^{-6}$ are given in [11]. In sections 2 and 3 number and phase properties [6–10] of the macrodeformed $|z\rangle_q$ states are respectively analysed. In section 4 and appendix C, the associated standard number-and-phase uncertainty relations [7, 10] are treated. Section 5 contains several concluding remarks.

2. Number properties

2.1. q-oscillator commutation relations and CSs

In the Heisenberg representation, we consider a specific mode of the q-analogue radiation field having a specific polarization $\hat{\epsilon}$ where for q real

$$aa^\dagger - q^{\pm 1/2}a^\dagger a = q^{\mp N/2} \tag{2}$$

with N the number operator, and with $[N, a^\dagger] = a^\dagger$, $[N, a] = a$, and $[a, a] = 0$. We suppress both the subscript $\boldsymbol{k}$ and the polarization vectors $\hat{\epsilon}$ for the q-analogue electric and magnetic fields, etc.

In the $|n\rangle_q$ occupation number basis, $\langle m|n\rangle = \delta_{mn}$, and

$$a^\dagger|n\rangle = \sqrt{[n+1]}|n+1\rangle \qquad a|n\rangle = \sqrt{[n]}|n-1\rangle \tag{3}$$

with the q-boson vacuum $|0\rangle_q$ such that $a|0\rangle_q = 0$. Normally we will suppress the q subscript on the number basis states, etc. Besides N, there are two q-deformed number-like operators $[N]$ and $[N+1]$ with

$$\begin{aligned} a^\dagger a|n\rangle &= [N]|n\rangle = [n]|n\rangle \\ aa^\dagger|n\rangle &= [N+1]|n\rangle = [n+1]|n\rangle. \end{aligned} \tag{4}$$

The 'bracket number' is defined by

$$\begin{aligned} [x] &\equiv \frac{q^{x/2} - q^{-x/2}}{q^{1/2} - q^{-1/2}} \\ &\equiv \frac{\sinh\{(x \ln q)/2\}}{\sinh\{(\ln q)/2\}} \end{aligned} \tag{5}$$

and $[x]$ is invariant under $q \leftrightarrow 1/q$. So without loss of generality, for q real it suffices to fix $0 < q \leqslant 1$ and to study the macrodeformed region by letting $q \to 0$.

The q-analogue CSs satisfy

$$a|z\rangle_q = z|z\rangle_q \tag{6}$$

where z is a complex number, $z = |z|e^{i\theta}$. Up to a phase choice,

$$|z\rangle_q = N(z) \sum_{n=0}^{\infty} \frac{z^n}{\sqrt{[n]!}} |n\rangle_q \tag{7}$$

where $N(z) = e_q(|z|^2)^{-1/2}$. The q-exponential function [5] is defined by the absolutely and uniformly convergent power series

$$e_q(z) = \sum_{n=0}^{\infty} \frac{z^n}{[n]!} \tag{8}$$

where $[n]! = [n][n-1]\ldots[1], [0]! = 1$. Sum rules of the reciprocals of the zeros of $e_q(z)$ play a role in expansions of q-analogue special functions analogous to that of the Bernoulli numbers in ordinary series expansions†.

Throughout this paper all expectation values will be in the CS basis

$$\langle \hat{O} \rangle \equiv {}_q\langle z|\hat{O}|z\rangle_q \tag{9}$$

unless noted otherwise.

2.2. Stair function behaviour of $\langle z|N|z\rangle$ in macrodeformed region

In the CS basis, the expectation value of the number operator, N, is

$$\langle z|N|z\rangle = e_q(|z|^2)^{-1} \sum_{n=0}^{\infty} \frac{|z|^{2n} n}{[n]!} \tag{10}$$

whereas for the deformed number operator it is

$$\langle z|[N]|z\rangle = |z|^2. \tag{11}$$

For convenience, figures in the present paper are shown against $|z|^2$, or against $\log(|z|^2) \equiv \log_{10}(|z|^2)$. In investigating the region of macro q-deformation, we hold $|z|^2$ fixed and take $q \to 0$; in the figures we set $q = 10^{-15}$ (for 10^{-6} see [11]).

Much of the simple behaviour which occurs in the macrodeformed region can be understood because the macrodeformed CSs are actually 'pseudo-Fock states'; while it is essential to include all number basis components in the expansion of $|z\rangle_q$ so as to satisfy

$$a|z\rangle_q = z_q|z\rangle_q \tag{12}$$

† For instance, for p complex, in analogy to the Riemann zeta function one can define for $e_q(z)$

$$\zeta_e(p) \equiv \sum_{i=1}^{\infty} \left(\frac{1}{z_i}\right)^p$$

where z_i are the zeros of $e_q(z)$. Then for $|z| < |z_1|$,

$$\ln\{e_q(z)\} = -\sum_{n=1}^{\infty} \frac{1}{n} \zeta_e(n) z^n.$$

Compare equations (56)–(59) in [5]. As $q \to 0$, there is the asymptotic formula $\zeta_e(p) \to \exp(\iota\pi p)\{1-q^{p/2}\}^{-1}(1-q)^p$ whereas for $E_q(z)$ for $q > 1$ there is $\zeta_E(p) = \exp(\iota\pi p)\{q^p - 1\}^{-1}(q-1)^p$.

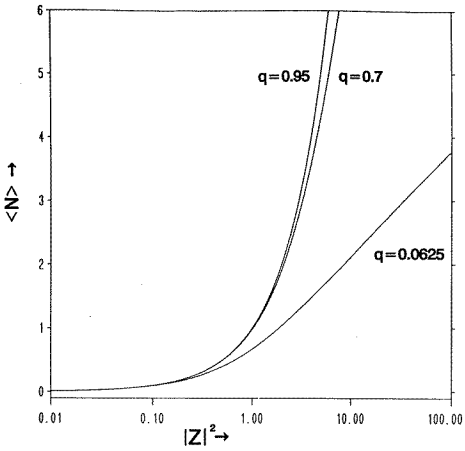

Figure 1. Behaviour of the mean value of the number operator $\langle N\rangle \equiv {}_q\langle z|N|z\rangle_q$ as $|z|^2$ varies for fixed q in the region $\frac{1}{16} \leqslant q < 1$. For ordinary bosons ($q = 1$), there is a linear $\langle N\rangle = |z|^2$, instead of the approximately logarithmic $\log(|z|^2)$ dependence, equation (32), for $q \neq 1$. The next two figures show what occurs for macro q-deformation, i.e. as $q \to \infty$ (equivalently, as $q \to 0$).

nevertheless, in evaluating CS expectation values, $\langle z|\hat{O}|z\rangle$, one or two Fock components frequently dominate as $q \to 0$. For instance, figures 1–3 indicate that such a dominance is occurring because in the region of macrodeformation

$$\langle z|N|z\rangle \approx \boldsymbol{S}_q(\log(|z|^2)) \tag{13}$$

i.e. the mean value of N approaches a 'stair function' $\boldsymbol{S}_q(\log|z|^2)$ (see appendix A).

In particular, using $[x]$ we define $|z|^2$ values for 'step' states

$$|z_s|^2 \equiv [s + \tfrac{1}{2}] \qquad s = 0, 1, 2, \ldots$$
$$\approx \begin{cases} \dfrac{q^{-(2s-1)/4}}{(1-q)} & s \neq 0 \\ (q^{-1/4} + q^{1/4})^{-1} & s = 0 \end{cases} \tag{14}$$

and for 'riser' states

$$|z_r|^2 \equiv [r + 1] \qquad r = 0, 1, 2, \ldots$$
$$\approx \begin{cases} \dfrac{q^{-r/2}}{(1-q)} & r \neq 0 \\ 1 & r = 0. \end{cases} \tag{15}$$

More precisely, one would refer to the $|z_r\rangle$ states of equation (15) as 'mid-riser' states, for instance 'quarter-riser' states $|z_b\rangle$ with $|z_b|^2 = [b + \frac{3}{4}]$, $b = 1, 2, \ldots$, can be introduced (see appendices C and D).

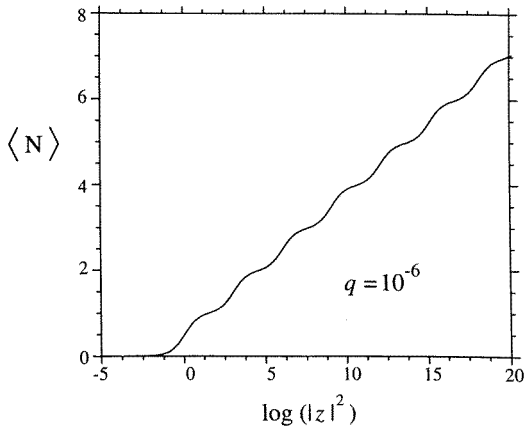

Figure 2. Behaviour of $\langle N \rangle$ for fixed $q = 10^{-6}$. Because of the manifest $q \leftrightarrow 1/q$ symmetry, without loss of generality we can consider $0 < q \leqslant 1$. (On the horizontal axis, the symbol log represents $\log_{10}$, i.e. logarithms to the base 10.)

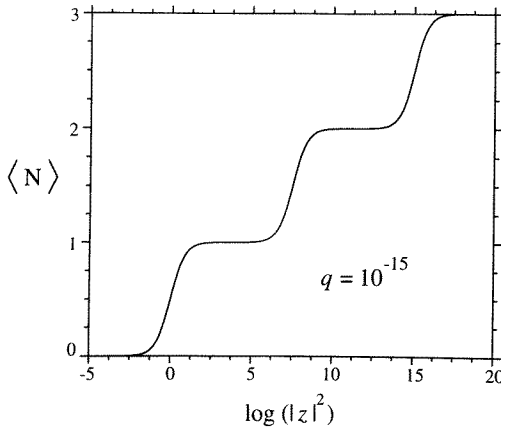

Figure 3. Behaviour of $\langle N \rangle$ for fixed $q = 10^{-15}$. The following figures are all for this smaller q value because the dominant signatures, e.g. $\langle N \rangle$ has approximately a 'stair function' dependence on $\log(|z|^2)$ per equation (13), are more visible for $q = 10^{-15}$ (for $q = 10^{-6}$ see [11]). For $\log(|z|^2)$ negative, there is a flat 'landing' with $\langle N \rangle \simeq 0$. Notice that the first 'step' is labelled by the first positive integer, $s = 1$, since $\langle N \rangle|_{|z_s\rangle} \simeq s$ for each step.

This stair function† behaviour as $q \to 0$ can also be shown analytically by the methods in [5]. When q is small or n large, the deformation of n can be approximated,

$$[n] = \frac{q^{(1-n)/2} - q^{(1+n)/2}}{(1-q)} \approx \frac{q^{(1-n)/2}}{(1-q)} \tag{16}$$

† Figure 3 has the same structure as that observed in the quantum Hall effect in the plot of the normalized inverse Hall resistance ($h/e^2 R_{\mathrm{H}}$) against the normalized ratio (nhc/eB) of the electron number density and the magnetic field. For example, figure 3 can be compared with figure 1.2 of [12]. The longitudinal resistance, R_{L}, has a similar structure to that of $I_1(|z|)$ displayed later in figure 5.

and

$$[n]! = \frac{q^{-n(n-1)/4}}{(1-q)^n}\{(1-q)(1-q^2)\dots(1-q^n)\}$$
$$\approx \frac{q^{-n(n-1)/4}}{(1-q)^n} \tag{17}$$

which is the analogue of the Stirling approximation of $n!$. The last lines in equations (14) and (15) follow by equation (16).

So from equation (7), associated with equations (14) and (15), are the 'approximate Fock states for $|z_s\rangle$ and $|z_r\rangle$'

$$|z_s\rangle \underset{q\to 0}{\longrightarrow} \mathrm{e}^{\mathrm{i}s\theta}|s\rangle \tag{18}$$

with

$$\langle N\rangle|_{|z_s\rangle} \to s \qquad \Delta N|_{|z_s\rangle} \to 0$$

and

$$|z_r\rangle \underset{q\to 0}{\longrightarrow} \frac{1}{\sqrt{2}}\mathrm{e}^{\mathrm{i}r\theta}\{|r\rangle + \mathrm{e}^{\mathrm{i}\theta}|r+1\rangle\} \tag{19}$$

with

$$\langle N\rangle|_{|z_r\rangle} \to r + \tfrac{1}{2} \qquad \Delta N|_{|z_r\rangle} \to \tfrac{1}{2}.$$

Note that there is a fixed phase relation, determined by $\theta = \arg(z)$, between the two dominant states in $|z_r\rangle$. Such a dominance, for a fixed $|z|^2$ region, by a few terms in the series also occurs for the q-exponential function $e_q(|z|^2)$, see section 2 of [5]. This dominance property is not surprising since a zero-order entire function will possess polynomial-type behaviour. An improved approximation would be to successively include additional adjacent terms, as $|r-1\rangle$ and $|r+2\rangle$ components in equation (19) for the (mid)riser state, etc.

Analytically, by the approximation of equation (17) we obtain directly from equation (10) the leading order in q corrections: for the step values ($s > 0$)

$$e_q(|z_s|^2) = \sum_{n=0}^{\infty}\frac{[s+\frac{1}{2}]^n}{[n]!}$$
$$= \frac{[s+\frac{1}{2}]^s}{[s]!}\sum_{n=0}^{\infty}[s+\tfrac{1}{2}]^{n-s}\frac{[s]!}{[n]!}$$
$$\underset{q\to 0}{\longrightarrow} \frac{[s+\frac{1}{2}]^s}{[s]!}\{1+2q^{1/4}+2q+\mathcal{O}(q^{9/4})\} \tag{20}$$

and

$$\sum_{n=0}^{\infty}\frac{[s+\frac{1}{2}]^n n}{[n]!} \underset{q\to 0}{\longrightarrow} \frac{s[s+\frac{1}{2}]^s}{[s]!}\{1+2q^{1/4}+2q+\mathcal{O}(q^{9/4})\} \tag{21}$$

so

$$\langle N\rangle|_{|z_s\rangle} = e_q(|z_s|^2)^{-1}\sum_{n=0}^{\infty}\frac{[s+\frac{1}{2}]^n n}{[n]!}$$
$$\underset{q\to 0}{\longrightarrow} s\{1+\mathcal{O}(q^{5/4})\} \qquad s > 0 \tag{22}$$

where the possible $\mathcal{O}(q^{1/4})$ and $\mathcal{O}(q)$ corrections have cancelled. (The $\mathcal{O}(q^{5/4})$ correction in equation (22) arises because the approximation of equation (17) neglects $\mathcal{O}(q)$ corrections from the braces factor in the first line.) Similarly, for the 'riser' $|z_r|^2$ values for $r > 0$,

$$e_q(|z_r|^2) \quad \underset{q\to 0}{\longrightarrow} \frac{[r+1]^r}{[r]!}\{\cdots + q^{1/2} + 1 + 1 + q^{1/2} + \cdots\}$$

$$\underset{q\to 0}{\longrightarrow} \frac{[r+1]^r}{[r]!} 2\{1 + q^{1/2} + \mathcal{O}(q^{3/2})\} \tag{23}$$

$$\sum_{n=0}^{\infty} \frac{[r+1]^n}{[n]!} \underset{q\to 0}{\longrightarrow} \frac{[r+1]^r}{[r]!} 2(r+\tfrac{1}{2})\{1 + q^{1/2} + \mathcal{O}(q^{3/2})\} \tag{24}$$

so

$$\langle N\rangle|_{|z_r\rangle} \underset{q\to 0}{\longrightarrow} (r+\tfrac{1}{2})\{1 + \mathcal{O}(q^{3/2})\} \qquad r > 0 \tag{25}$$

where the possible $\mathcal{O}(q^{1/2})$ corrections cancel.

Next, for the variances of the number operator in the CS basis

$$(\Delta N)^2 = \langle N^2\rangle - \langle N\rangle^2 \tag{26}$$

we obtain by using equation (17)

$$(\Delta N)^2|_{|z_s\rangle} \underset{q\to 0}{\longrightarrow} 2q^{1/4} \tag{27}$$

$$(\Delta N)^2|_{|z_r\rangle} \underset{q\to 0}{\longrightarrow} \tfrac{1}{4} + 2q^{1/2}. \tag{28}$$

As shown in figure 4, the ratio of the variance to the mean value, $(\Delta N)^2/\langle N\rangle$, is very distinct [4] from that for Poisson statistics: for step states

$$\left.\frac{(\Delta N)^2}{\langle N\rangle}\right|_{|z_s\rangle} \underset{q\to 0}{\longrightarrow} \left\{\frac{4q^{1/2}}{s} \to 0 \qquad \text{for } s > 0\right\} \tag{29}$$

and for (mid)riser states

$$\left.\frac{(\Delta N)^2}{\langle N\rangle}\right|_{|z_r\rangle} \underset{q\to 0}{\longrightarrow} \frac{1}{2(2r+1)} \qquad \text{for } r > 0. \tag{30}$$

The approximately linear slope of $\langle N\rangle$ can be partially explained by a CS argument [4]. From

$$\langle N\rangle = \frac{2}{\ln q}\left\langle \sinh\left\{[N]\sinh\left\{\frac{\ln q}{2}\right\}\right\}\right\rangle \tag{31}$$

a diagonal CS replacement *for large* $|z|$ of $[N] \to \{\langle[N]\rangle = |z|^2\}$ yields

$$\langle N\rangle \to \alpha_q \log|z|^2 + \beta_q + \mathcal{O}(1/|z|^4) \tag{32}$$

with

$$\alpha_q = (\log q^{-1/2})^{-1}. \tag{33}$$

This value of α_q is a good approximation for the linear slopes displayed in figures 1–3. However, the value of β_q must be arbitrarily chosen depending on whether the series of points (connected by the linear line) are step and (mid)riser points, for which $\beta_q = \frac{1}{2}$, or 'quarter-riser' points $[z_b]^2 = [b + \frac{3}{4}]$, etc.

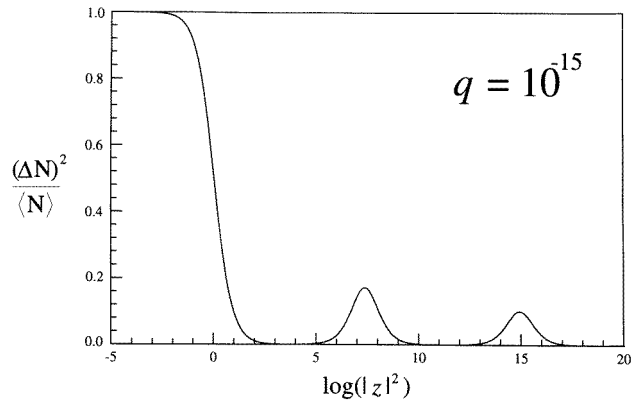

Figure 4. Behaviour of the ratio of the variance to the mean value, $(\Delta N)^2/\langle N\rangle$, as $|z|^2$ varies for fixed $q = 10^{-15}$. Also for $\frac{1}{16} \leqslant q < 1$, this ratio $(\Delta N)^2/\langle N\rangle \to 0$ as $|z|^2 \to \infty$, whereas for Poisson statistics, i.e. $q = 1$ CSs, $(\Delta N)^2/\langle N\rangle = 1$.

2.3. 'Jump in $\log(|z|^2)$*' behaviour of q-Poisson number distribution in macrodeformed region*

From the q-Poisson number distribution in the $|z\rangle_q$ basis,

$$\begin{aligned} P_q(n) &\equiv |\,{}_q\langle z|n\rangle_q|^2 \\ &= e_q(|z|^2)^{-1}\left\{\frac{|z|^{2n}}{[n]!}\right\} \end{aligned} \tag{34}$$

we obtain by equation (17) that at step $|z_s|^2$ values for $s > 0$

$$P_q(n)|_{|z_s\rangle} \underset{q\to 0}{\longrightarrow} \left(\frac{1}{1+2q^{1/4}}\right) \times \begin{cases} 1 & n = s \\ q^{k^2/4} & n = s \pm k \\ & k = 1, 2, \ldots. \end{cases} \tag{35}$$

Notice that the peak position in $P_q(n)|_{|z_s\rangle}$ 'jumps' as $\log(|z_s|^2)$ increases. This is, of course, consistent with the 'pseudo Fock-state' interpretation of figures 2 and 3.

At the riser values of $|z_r|^2$, we find

$$P_q(n)|_{|z_r\rangle} \underset{q\to 0}{\longrightarrow} \frac{1}{2(1+q^{1/2})} \times \begin{cases} 1 & n = r, r+1 \\ q^{1/2k(k+1)} & n = r-k \\ & k = 1, 2, \ldots, r \\ q^{1/2k'(k'-1)} & n = r+k' \\ & k' = 1, 2, \ldots. \end{cases} \tag{36}$$

Again, a 'jump' in the central two-peaks value occurs as $\log(|z_r|^2)$ is increased.

3. Phase properties

3.1. Definition of Fourier phase operators

The following phase operator definitions [4] hold both for ordinary bosons and bosonic quasi-particles ($q = 1$) and more generally for q-bosons ($q \neq 1$). The Susskind–Glogower (SG) Hermitian sine and cosine operators [6, 4], $\widehat{\cos}(\phi)$ and $\widehat{\sin}(\phi)$ correspond to

$a \equiv ([N+1])^{1/2}\widehat{\exp}(\mathrm{i}\phi)$ with $\widehat{\exp}(-\mathrm{i}\phi) \equiv \{\widehat{\exp}(\mathrm{i}\phi)\}^{\dagger}$. In the occupation number basis, this is equivalent to

$$\widehat{\exp}(\mathrm{i}\phi) = \sum_{n=0}^{\infty} |n\rangle\langle n+1|. \tag{37}$$

The Hermitian Fourier phase operators (FPOs) are defined [13] by

$$\begin{aligned} \widehat{\cos}(l\phi) &\equiv \frac{1}{2}\{(\widehat{\exp}(\mathrm{i}\phi))^{l} + (\widehat{\exp}(-\mathrm{i}\phi))^{l}\} \\ \widehat{\sin}(l\phi) &\equiv \frac{1}{2i}\{(\widehat{\exp}(\mathrm{i}\phi))^{l} - (\widehat{\exp}(-\mathrm{i}\phi))^{l}\} \end{aligned}. \tag{38}$$

For $z = |z|\mathrm{e}^{\mathrm{i}\theta}$, it follows as shown in [13] that there is a simple polar factorization of the expectation values of these FPOs in the CS basis:

$$\begin{aligned} {}_q\langle z|\widehat{\cos}(l\phi)|z\rangle_q &= \cos(l\theta) I_l(|z|) \\ {}_q\langle z|\widehat{\sin}(l\phi)|z\rangle_q &= \sin(l\theta) I_l(|z|) \end{aligned} \tag{39}$$

where the radial functions are

$$I_l(|z|) = |z|^l e_q(|z|^2)^{-1} \sum_{n=0}^{\infty} \frac{|z|^{2n}}{\sqrt{[n]![n+l]!}}. \tag{40}$$

Note [13] that q-deformation only directly affects the radial part (the Higgs modes) and not the phase part (the Nambu–Goldstone modes) of these FPO expectation values†.

These FPO equations (39) are exactly the same for the Pegg–Barnett Hermitian phase operator, $\hat{\phi}_q$ [7, 4]. $\hat{\phi}_q$ is defined in an $(s'+1)$-dimensional finite subspace

$$\hat{\phi}_q = \sum_{m=0}^{s'} \theta_m |\theta_m\rangle\langle\theta_m| \tag{41}$$

with

$$\begin{aligned} |\theta_m\rangle &= (s'+1)^{-1/2} \sum_{n=0}^{s'} \exp(\mathrm{i}n\theta_m)|n\rangle_q \\ \theta_m &= \theta_0 + \frac{2m\pi}{s'+1} \qquad m = 0, 1, \ldots, s' \end{aligned} \tag{42}$$

where θ_0 is an indicial reference phase. The limit $s' \to \infty$ is only to be taken after the matrix elements are calculated. Associated with $\hat{\phi}_q$ is the unitary

$$\exp(\mathrm{i}\hat{\phi}) \equiv |0\rangle\langle 1| + |1\rangle\langle 2| + \cdots + |s'-1\rangle\langle s'| + \exp\{\mathrm{i}(s'+1)\theta_0\}|s'\rangle\langle 0| \tag{43}$$

which only differs in the last term against equation (37) for the SG $\widehat{\exp}(\mathrm{i}\phi)$ operator.

Notice that the 'window' of eigenstates of the PB phase operator $\hat{\phi}_q$ lies between θ_0 and $\theta_0 + 2\pi$. Therefore, to avoid 'artifacts' due to the edges of the window [14], we choose the indicial phase

$$\theta_0 = \theta - \frac{\pi s'}{s'+1} \tag{44}$$

so that in the limit $s' \to \infty$, the 'window' is centred about the phase θ of the coherent state $|z\rangle$, $z = |z|\mathrm{e}^{\mathrm{i}\theta}$.

† q-deformation also only directly affects the radial part of the expectation values of $\cos\Phi$ and $\sin\Phi$ in the q-spin coherent states [15], see equation (19) in [16]. We thank Professor Zurong Yu for bringing this to our attention.

3.2. Simple phase properties in macrodeformed region

The reader should note that in subsection 3.2.2 we discuss the effects of macro q-deformation on two more intuitive phase quantities: the variance $(\Delta\hat{\phi}_q)^2$ and the normalized PB phase-distribution function

$$\bar{P}_q(\theta_m) \equiv \lim_{s'\to\infty} (s'+1)|\langle\theta_m|z\rangle|^2. \tag{45}$$

$\bar{P}_q(\theta_m)$ is the natural conjugate-variable analogue of the q-boson number distribution $P_n^q(z)$ discussed above, see equations (34)–(36). However, logic dictates that we begin by discussing the effects of macro q-deformation on the radial functions $I_l(|z|)$ for we need some of these results to treat $(\Delta\hat{\phi}_q)^2$ and $\bar{P}_q(\theta_m)$.

3.2.1. Properties of the radial functions $I_l(|z|)$ for $q \neq 1$. Again by using the approximation of equations (16) and (17) we find at the step values $|z_s|^2$

$$I_1(|z_s|) \underset{q\to 0}{\longrightarrow} 2q^{1/8}\{1-2q^{1/4}\} \qquad s \geqslant 1 \tag{46}$$

and for $l \geqslant 2$ and $s \geqslant 1$

$$I_l(|z_s|) \underset{q\to 0}{\longrightarrow} q^{l^2/8}\left\{\sum_{k=1}^{s} q^{k/4(k-l)} + 1\right\}\{1-2q^{1/4}\} \tag{47}$$

so

$$I_2(|z_s|) \underset{q\to 0}{\longrightarrow} q^{1/4}(1+\mathcal{O}(q)) \qquad s \geqslant 1. \tag{48}$$

Likewise, at the riser $|z_r|^2$ values, we obtain

$$I_1(|z_r|) \underset{q\to 0}{\longrightarrow} \tfrac{1}{2}\{1+2q^{1/4}\} \qquad r \geqslant 1 \tag{49}$$

and for $l \geqslant 2$ and $r \geqslant 1$,

$$I_l(|z_r|) \underset{q\to 0}{\longrightarrow} \frac{1}{2}q^{l(l-1)/8}\left\{\sum_{k=1}^{r} q^{k(k-l+1)/4} + 1 + q^{l/4}\right\}\{1-q^{1/2}\} \tag{50}$$

so

$$I_2(|z_r|) \to q^{1/4}\{1+\mathcal{O}(q)\} \qquad r \geqslant 2. \tag{51}$$

The first- and second-order radial functions are especially important because for $q \neq 1$ in the $|z\rangle_q$ semi-classical limit where $|z| \to \infty$, all the odd (even) orders of $I_l(|z|)$ can be respectively written

$$I_{l(\text{odd})} \approx q^{(l^2-1)/16} I_1(|z|) \tag{52}$$

$$I_{l(\text{even})} \approx q^{(l^2-4)/16} I_2(|z|) \tag{53}$$

as is shown in appendix B. For $q \neq 1$ the function $I_1(|z|)$ oscillates as $\log(|z|^2)$ increases, see figure 5. By equation (52), all odd orders $I_{l(\text{odd})}$ also must oscillate (for $|z|^2$ large enough) albeit with much decreased amplitudes. For $q \neq 1$, as shown in [4], $I_2(|z|)$ does not oscillate, but rather approaches the limit $q^{1/4}$ as $z \to \infty$; hence, by equation (53), $I_{l(\text{even})}(|z|) \to q^{l^2/16}$ as $z \to \infty$.

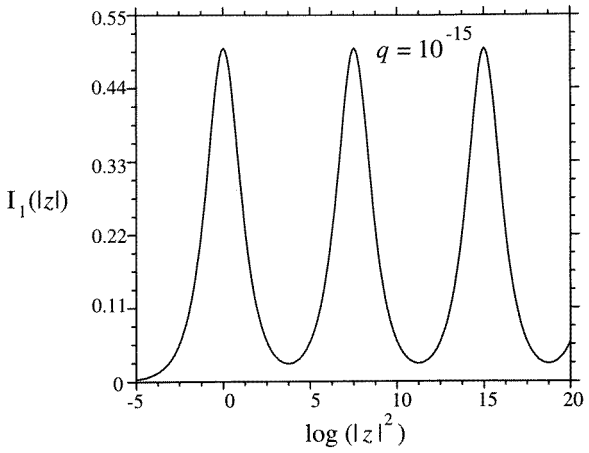

Figure 5. For $q = 10^{-15}$, the oscillatory behaviour of the first radial function $I_1(|z|)$. For arbitrary q and $|z|$ values, ${}_q\langle z|\cos(\hat{\phi}_q)|z\rangle_q = \cos\theta I_1(|z|)$ and ${}_q\langle z|\sin(\hat{\phi}_q)|z\rangle_q = \sin\theta I_1(|z|)$ for the q-analogue PB phase operator $\hat{\phi}_q$, and also for the SG Hermitian operators $\widehat{\cos}(\phi)$ and $\widehat{\sin}(\phi)$. q-deformation only affects the radial part, and not the polar part of expectation values of Fourier phase operators in the CS basis [13].

3.2.2. Properties of $(\Delta\hat{\phi}_q)^2$ and of $\bar{P}_q(\theta_m)$ in macrodeformed region. The variance of the PB phase operator, $\hat{\phi}_q$, can be written completely in terms of the radial functions

$$(\Delta\hat{\phi}_q)^2 = \frac{\pi^2}{3} + 4e_q(|z|^2)^{-1}\sum_{n>l}^{\infty}\frac{(-1)^{n+l}}{(n-l)^2}\frac{|z|^{n+l}}{\sqrt{[n]![l]!}}$$
$$= \frac{\pi^2}{3} + 4\sum_{l=1}^{\infty}\frac{(-)^l}{l^2}I_l(|z|). \tag{54}$$

So by equations (52) and (53), $I_1(|z|)$ will dominate for $|z|^2$ large; thus

$$(\Delta\hat{\phi}_q)^2 \to \begin{cases} \dfrac{\pi^2}{3} - 8q^{1/8} & \text{at } |z_s|,\ s \geqslant 1 \\ \dfrac{\pi^2}{3} - 2 & \text{at } |z_r|,\ r \geqslant 1. \end{cases} \tag{55}$$

As $|z| \to 0$, $(\Delta\hat{\phi}_q)^2 \to \pi^2/3$ for all q.

So for the step values, $(\Delta\hat{\phi}_q)^2 \approx \pi^2/3$ which corresponds to what is expected classically for a state of random phase. This agrees with the 'pseudo Fock-state' interpretation of the step $|z_s\rangle$ CSs since a pure number state also gives $(\Delta\hat{\phi}_q)^2|_{|n\rangle} = \pi^2/3$. for $q = 10^{-15}$, figure 6 shows how $(\Delta\hat{\phi}_q)^2$ behaves as $|z|^2$ varies between the step and riser values. (For $q = 10^{-6}$, the $|z_s|$ peaks' values of $(\Delta\hat{\phi}_q)^2|_{|z_s\rangle} \simeq (\pi^2/3 - 1.42)$ is noticeably lower than the maximum for $\log|z|^2 < 0$.)

The normalized PB phase-distribution can also be written completely in terms of the radial functions

$$\bar{P}_q(\theta_m) = \lim_{s'\to\infty}(s'+1)|\langle\theta_m|z\rangle|^2$$
$$= 1 + 2\sum_{l=1}^{\infty}\cos\{l(\theta-\theta_m)\}I_l(|z|). \tag{56}$$

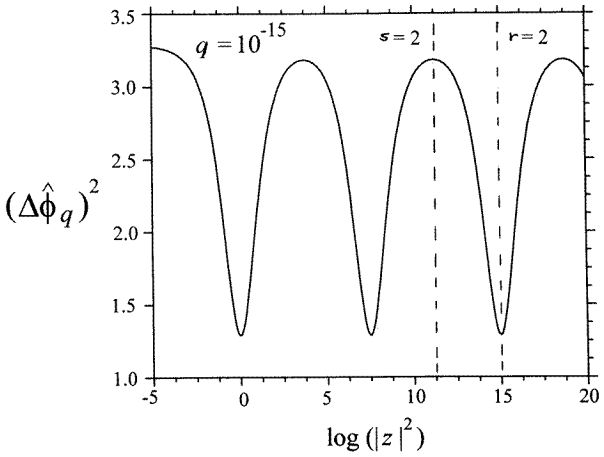

Figure 6. Behaviour of the variance of $(\Delta\hat{\phi}_q)^2$ of the q-analogue Pegg–Barnett phase operator as $|z|^2$ varies for $q = 10^{-15}$. For comparison, note that for $\frac{1}{16} \leqslant q < 1$, this ratio $(\Delta\hat{\phi}_q)^2 \to\sim (1/2\eta_q)^2$ for $|z|^2 > 10$ where numerically $\eta_q \simeq$ (q-dependent constant), whereas for $q = 1$, $(\Delta\hat{\phi}_q)^2 \to 1/(4|z|^2)$ for $|z|^2 > 10$. In the limit $q \to 0$, at $|z_s\rangle$ values where $\langle N\rangle \simeq s$, $(\Delta\hat{\phi}_q)^2 \to \pi^2/3$ corresponding to completely random phase distribution; whereas at the $|z_r\rangle$ 'riser' values $(\Delta\hat{\phi}_q)^2 \to (\pi^2/3 - 2)$.

So for large $|z|$ values,

$$\bar{P}_q(\theta_m) \to \begin{cases} 1 + 4q^{1/8}\cos(\theta - \theta_m) & \text{at } |z_s|,\ s \geqslant 1 \\ 1 + \cos(\theta - \theta_m) & \text{at } |z_r|,\ r \geqslant 1. \end{cases} \tag{57}$$

For $q = 10^{-15}$, $4q^{1/8} = 0.053$ which characterizes the departure from a completely random, i.e. flat, distribution, see figure 7. (Note that for $q = 10^{-6}$, $4q^{1/8} = 0.71$ so then there is a very noticeable departure from randomness.)

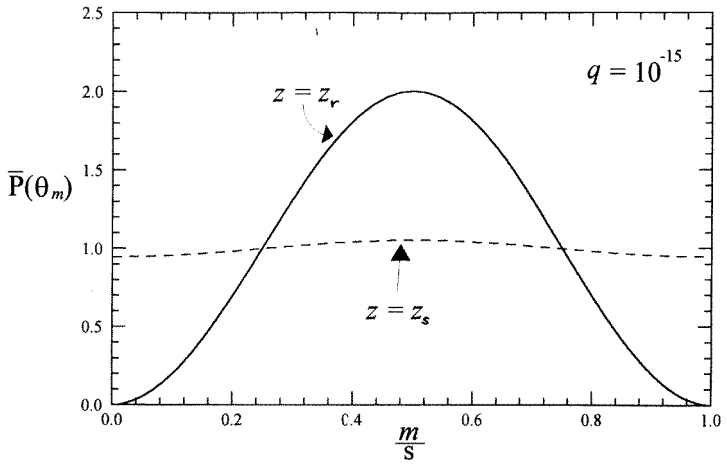

Figure 7. For $q = 10^{-15}$, the q-boson Pegg–Barnett normalized phase distribution function $\bar{P}_q(\theta_m)$, see equation (45), for the step $|z_s\rangle$ values and riser $|z_r\rangle$ values.

4. Number-phase uncertainty relation

For the PB phase operator, $\hat{\phi}_q$, there is the number-phase uncertainty relation [7, 4]

$$(\Delta N)^2(\Delta\hat{\phi}_q)^2 \geqslant \tfrac{1}{4}|\langle[N,\hat{\phi}_q]\rangle|^2. \tag{58}$$

For $\frac{1}{16} < q < 1$ it was shown in [4] that $[N,\hat{\phi}_q] \approx \mathrm{i}$ and that this uncertainty relation equation (58) is approximately minimized by the $|z\rangle_q$ CSs for $|z|^2 \geqslant 10$. However, with sufficient (extreme) numerical resolution, one discovers that for q near but not equal to 1, both sides of the uncertainty relation equation (58) actually oscillate. For instance, for $q = 10^{-1}$ the amplitude of the oscillation about $\frac{1}{4}$ in the region $\sim 2.5 < \log|z|^2$ is (amp.) $\sim 5 \times 10^{-14}$, with period in $(\log(|z|^2) \sim 0.5$ in agreement with equations (14) and (15).

In the region of macro q-deformation, we again evaluate both sides of equation (58) and find

$$(\Delta N)^2(\Delta\hat{\phi}_q)^2 \to \begin{cases} 2q^{1/4}\left(\dfrac{\pi^2}{3} - 8q^{1/8}\right) & \text{at } |z_s\rangle \\ \left(\dfrac{1}{4} + 2q^{1/2}\right)\left(\dfrac{\pi^2}{3} - 2\right) & \text{at } |z_r\rangle \end{cases} \tag{59}$$

$$\tfrac{1}{4}|\langle[N,\hat{\phi}_q]\rangle|^2 \to \begin{cases} q^{1/4} & \text{at } |z_s\rangle \\ \frac{1}{4}(1+2q^{1/4}) & \text{at } |z_r\rangle. \end{cases} \tag{60}$$

Consequently, for $q = 10^{-15}$ (as shown in figure 8) at the step values both sides of equation (58) approximately vanish as is expected since $|z_r\rangle \approx \mathrm{e}^{\mathrm{i}r\theta}|r\rangle$. At the riser values there is in contrast a finite gap of

$$\left\{(\Delta N)^2(\Delta\hat{\phi}_q)^2 - \frac{1}{4}|\langle[N,\hat{\phi}_q]\rangle|^2\right\}\Big|_{|z_r\rangle} \underset{q\to 0}{\longrightarrow} \frac{3}{4}\left\{\left(\frac{\pi}{3}\right)^2 - 1\right\} \tag{61}$$

so N and $\hat{\phi}_q$ are no longer 'almost canonically conjugate operators' in the region of macro q-deformation. (For $q = 10^{-6}$, the range of the oscillatory behaviour is somewhat different [11] (against figure 8) in that there is a finite separation between the two curves which varies between 0.01 and 0.05 as $\log(|z|^2)$ increases with $\frac{1}{4}|\langle[N,\hat{\phi}_q]\rangle|^2 >\sim 0.09$ for all $\log(|z|^2) >\sim 1$.)

In appendix C, we discuss the properties of the Carruthers–Nieto (number-phase) uncertainty relations in the macrodeformed region for both the SG and the PB phase operators.

5. Concluding remarks

5.1. Commutation relations and $q \leftrightarrow 1/q$ symmetry

The basic q-boson commutation relations

$$aa^\dagger - q^{\pm 1/2}a^\dagger a = q^{\mp N/2} \tag{62}$$

and q-deformed bracket $[x]$ are both symmetric under $q \leftrightarrow 1/q$. Equivalent to equations (62), one has the two equations

$$a^\dagger a = [N] \qquad aa^\dagger = [N+1]. \tag{63}$$

In the bosonic $q \to 1$ limit equations (63) reduce directly to the usual bosonic $N \equiv a^\dagger a$ and $aa^\dagger = a^\dagger a + 1$. So the two equations (62) codify a specific one-parameter generalization

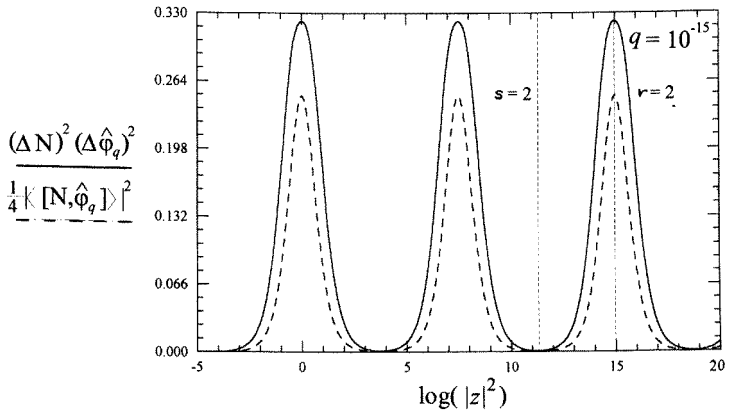

Figure 8. For $q = 10^{-15}$, behaviour of both sides of the uncertainty-relation inequality $(\Delta N)^2(\Delta\hat{\phi}_q)^2 \geqslant \frac{1}{4}|\langle[N, \hat{\phi}_q]\rangle|^2$ as $\log(|z|^2)$ increases.

(or deformation) of the definition of the number operator *and* the bosonic commutation relation†.

However, q-boson statistics are more than simply a one-parameter generalization: they are statistics which are also invariant under a discrete symmetry, $q \leftrightarrow 1/q$. The treatment of macro q-deformation in the present paper, for instance, preserves this $q \leftrightarrow 1/q$ invariance, and so, when one sets $q = 10^{-15}$ for a plot, this is mentally not to be distinguished from setting $q = 10^{15}$. In nature, it may be that $q \leftrightarrow 1/q$ invariance is not exact but is broken in one or more ways, much like nature breaks symmetries of other quantum mechanical models such as in exploiting the azimuthal quantum number, m, to break the intrinsic rotational invariance and space-inversion invariance (parity) of the mathematical formulation for the Schrödinger hydrogen atom or for the Heisenberg ferromagnet.

5.2. Fractional uncertainties and measurability of macrodeformed signatures

In [4] it was shown that in the CS basis the fractional uncertainties for most canonical operators (momentum, position, amplitude, phase) which characterize the quantum field go as

$$\lim_{|z|\to\infty} \frac{\Delta\hat{O}}{\langle\hat{O}\rangle} \to\sim \frac{\lambda^{1/2}(|z|)}{|z|} \tag{64}$$

in the $|z\rangle_q$ 'classical limit' where $|z|$ is large, and that for all z values the q-boson resolution function appearing in equation (64)

$$\lambda(z) = (q^{-1/2} - 1)|z|^2 + \{e_q(q^{1/2}|z|^2)/e_q(|z|^2)\}. \tag{65}$$

So for $0 < q < 1$, i.e. for the macrodeformed region,

$$\lim_{|z|\to\infty} \frac{\Delta\hat{O}}{\langle O\rangle} \to \{\sim q^{-1/4} \gg 1\} \tag{66}$$

† In the 'b' representation, $bb^\dagger - qb^\dagger b = 1$ and $[N]_b \equiv b^\dagger b$ where $[x]_b \equiv (1 - q^x)/(1 - q)$. Thus, in the macrodeformed region, $q \gg 1$, $[x]_b \approx q^{x-1}$, whereas from equation (5) for the 'a' representation of equations (62), $[x] \approx q^{(x-1)/2}$. Hence, the results obtained in the present paper also follow in the 'b' representation; in particular $\langle z|N_b|z\rangle$ displays a stair function behaviour for $q \gg 1$.

unlike for ordinary bosons in the CS basis. However, since the difference in adjacent steps in figures 2 and 3, etc. go as

$$|z_{s+1}|^2 - |z_s|^2 \to\sim q^{-1/2} \tag{67}$$

in an actual experiment the number signatures displayed in the equations and figures in this paper are expected not to be entirely masked, though smeared, by this more-quantum-like behaviour of $\Delta\hat{O}$ for $q \neq 1$.

In this context it perhaps should be emphasized that while for simplicity the figures in this paper present the stair function and other signatures of macro q-deformation for small mean values of $\langle N\rangle$ and small $\log(|z|^2)$ values, the same signatures hold analytically for orders of magnitude larger values. In which case there is stronger physical justification for the reliability of treating cooperative quasi-particle behaviour by a CS description since in successful CS applications to known physical bosonic systems both $|z|$ and $\langle z|N|z\rangle$ are large.

5.3. Macrodeformed model

The most remarkable outcome of analysing the $q \to 0$ limit of the q-bosonic commutation relations, equations (62), is that it provides, at least, a simple mathematical model which combines features from two distinct physical regions in the ordinary bosonic case: one a quantum mechanical limit with $|n\rangle$ states and other a semi-classical limit with $|z\rangle$ states with $|z|$ large. For macro q-deformation, on the one hand, the step $|z_s\rangle$ and (mid)riser states $|z_r\rangle$ do have a simple approximate Fock description, but yet to satisfy the basis CS requirement that $a|z\rangle_q = z|z\rangle_q$, every $|z\rangle_q$ coherent state must still have a component in each occupation state. The quantum-mechanical price of this decreased uncertainty in the mean number of particles

$$\lim_{|z|\to\infty} \frac{(\Delta N)^2}{\langle N\rangle} \to 0 \tag{68}$$

when q departs from unity is the greater fractional uncertainties of the other canonical physical quantities describing the quantum field theoretic system.

5.4. Role of deformation parameter 'q'

In the limit $q \to 0$, the stair function $\boldsymbol{S}_q(\log(|z|^2)) \to \Theta(\log(|z|^2))$, the Heaviside step function, which is a fermionic 'coherent state' system [17] since $\langle N\rangle = 0$ or 1. Also, $I_1(|z|) \to |z|/(1+|z|^2)$ and $I_l(|z|) \to 0$, $l \geqslant 2$.

Note that this limit is not taken at the creation and annihilation operator level, rather the limit is at the coherent state level. This behaviour of $\langle N\rangle$ is consistent with the observation that as $q \to 0$

$$|z\rangle \approx N(z)\left(|0\rangle + \frac{z}{[1]!}|1\rangle + \text{negligible}\right) \tag{69}$$

$$\longrightarrow \left(\frac{1}{1+|z|^2}\right)^{1/2}(|0\rangle + z|1\rangle) \tag{70}$$

since $[n] \to \infty$ for $n \geqslant 2$. The manifest $q \leftrightarrow 1/q$ symmetry is lost, however, in the second expression, equation (70). Note that due to manifest $q \leftrightarrow 1/q$ symmetry, there is only *one* fermionic $|z\rangle_q$ in the macrodeformed limit, i.e. not 'two' such states.

Thus, the role of the deformation parameter q, and of the associated concept of q-bosons, is to enable a simple and smooth interpolation between the classic bosonic *coherent states* ($q = 1$) and the fermionic *coherent states* ($q = \infty$ or 0).

Acknowledgments

This work was partially supported by US Department of Energy, Contract No DE-FG02-96ER40291. We wish to thank M G Gartley for helpful discussions.

Appendix A. A 'stair' functional

Using the Heaviside step functional, $\Theta(x')$, it is simple to introduce a 'stair' functional

$$\boldsymbol{S}(a, b, c; x) \equiv a \sum_{l=0}^{\infty} \Theta(x - lb - c) \tag{A1}$$

so that for $q <\sim 10^{-6}$

$$\langle N \rangle \equiv \langle z|N|z\rangle \approx \boldsymbol{S}_q(\log(|z|^2)). \tag{A2}$$

Here, in equation (A2),

$$\boldsymbol{S}_q(x) \equiv \boldsymbol{S}(1, -\tfrac{1}{2}\log q, 0; x) \tag{A3}$$

with

$$\begin{aligned} c &= 0 && \text{(beginning of first step)} \\ b &= \log(|z_{s=1}|^2) && \text{(length of each step)} \\ &= \log([2]) \simeq -\tfrac{1}{2}\log q \\ a &= 1 && \text{(height of each step).} \end{aligned}$$

Appendix B. Bifurcation in the structure of the radial functions $I_l(|z|)$ for l(odd) and l(even) when $q \neq 1$

For $q \neq 1$, we respectively define $\psi_{m(\text{odd})}(|z|)$ and $\psi_{n(\text{even})}(|z|)$ by

$$\begin{aligned} \psi_m(|z|) &= \sum_{r=0}^{\infty} \frac{|z|^{2(r+(m-1)/2)}}{[r]!\sqrt{[r+m]!/[r]!}} && m(\text{odd}) > 1 \\ \psi_n(|z|) &= \sum_{r=0}^{\infty} \frac{|z|^{2(r+(n-2)/2)}}{[r]!\sqrt{[r+n]!/[r]!}} && n(\text{even}) > 2 \end{aligned} \tag{B1}$$

so

$$\begin{aligned} I_m(|z|) &= |z| e_q(|z|^2)^{-1} \psi_m(|z|) \\ I_n(|z|) &= |z|^2 e_q(|z|^2)^{-1} \psi_n(|z|). \end{aligned}$$

We change variables to the positive integers α and β:

$$\alpha = \begin{cases} \dfrac{m-1}{2} & m \text{ odd} \\ \dfrac{n-2}{2} & n \text{ even} \end{cases}$$

$$\beta = r + \alpha.$$

Thereby,

$$\psi_m(|z|) = \sum_{\beta=\alpha}^{\infty} \frac{|z|^{2\beta}}{[\beta]!\sqrt{[\beta+1]}} \sqrt{\left(\frac{[\beta]![\beta+1]}{[\beta+\alpha+1]!}\right)\left(\frac{[\beta]!}{[\beta-\alpha]!}\right)}$$
$$= \sum_{\beta=\alpha}^{\infty} \frac{|z|^{2\beta}}{[\beta]!\sqrt{[\beta+1]}} \sqrt{\frac{[\beta]}{[\beta+\alpha+1]}\frac{[\beta-1]}{[\beta+\alpha]}\cdots\frac{[\beta-\alpha+1]}{[\beta+2]}}$$
$$\approx q^{1/4\alpha(\alpha+1)} \sum_{\beta=\alpha}^{\infty} \frac{|z|^{2\beta}}{[\beta]!\sqrt{[\beta+1]}} \tag{B2}$$

and

$$\psi_n(|z|) = \sum_{\beta=\alpha}^{\infty} \frac{|z|^{2\beta}}{[\beta]!\sqrt{[\beta+2][\beta+1]}} \sqrt{\left(\frac{[\beta]![\beta+1]}{[\beta+\alpha+2]!}\right)\left(\frac{[\beta]![\beta+2]}{[\beta-\alpha]!}\right)}$$
$$= \sum_{\beta=\alpha}^{\infty} \frac{|z|^{2\beta}}{[\beta]!\sqrt{[\beta+2][\beta+1]}} \sqrt{\frac{[\beta]}{[\beta+\alpha+2]}\frac{[\beta-1]}{[\beta+\alpha+1]}\cdots\frac{[\beta-\alpha+1]}{[\beta+3]}}$$
$$\approx q^{1/4\alpha(\alpha+2)} \sum_{\beta=\alpha}^{\infty} \frac{|z|^{2\beta}}{[\beta]!\sqrt{[\beta+2][\beta+1]}} \tag{B3}$$

by the identity

$$\frac{[l+x]}{[l+y]} \approx q^{(y-x)/2} \tag{B4}$$

which holds for large l and small q. So

$$I_{l(\text{odd})}(|z|) \approx q^{(l^2-1)/16}\{I_1(|z|) - e_q(|z|^2)^{-1}\mathfrak{P}_l^{(1)}(|z|)\}$$
$$\mathfrak{P}_l^{(1)}(|z|) \equiv \sum_{r=0}^{(l-3)/2} \frac{|z|^{2r+1}}{[r]!\sqrt{[r+1]}} \qquad l(\text{odd}) > 1 \tag{B5}$$

and

$$I_{l(\text{even})}(|z|) \approx q^{(l^2-4)/16}\{I_2(|z|) - e_q(|z|^2)^{-1}\mathfrak{P}_l^{(2)}(|z|)\}$$
$$\mathfrak{P}_l^{(2)}(|z|) \equiv \sum_{r=0}^{(l-4)/2} \frac{|z|^{2r+2}}{[r]!\sqrt{[r+2][r+1]}} \qquad l(\text{even}) > 2 \tag{B6}$$

where $\mathfrak{P}_l^{(1)}$ and $\mathfrak{P}_l^{(2)}$ are $\mathcal{O}(|z|^{l-2})$ polynomials. For finite $|z|$, corrections to equation (B4) can be important.

Appendix C. Behaviour of Carruthers–Nieto number-phase uncertainty relations as $q \to 0$

The Carruthers–Nieto uncertainty relations [10] were originally derived for the SG phase operators. However, as shown below, for $|z|^2$ sufficiently large, the differences in applying these uncertainty relations to the PB and SG case are in fact negligible because such differences go as $e_q(|z|^2)^{-1}$.

C.1. $Q(|z|,\theta)$

For $z = |z|e^{i\theta}$, there is the θ-dependent uncertainty relation

$$Q(|z|,\theta) = \frac{(\Delta\hat{N})^2(\Delta\widehat{\sin}(\phi))^2}{|\langle\widehat{\cos}(\phi)\rangle|^2} \geqslant \frac{1}{4} \tag{C1}$$

with

$$(\Delta\widehat{\sin}(\phi))^2 = \langle\{\widehat{\sin}(\phi)\}^2\rangle - (\langle\widehat{\sin}(\phi)\rangle)^2$$

where in the SG case

$$\begin{aligned}\langle\{\widehat{\sin}(\phi)\}^2\rangle &= \tfrac{1}{2} - \tfrac{1}{2}\cos(2\theta)I_2(|z|) - \tfrac{1}{4}e_q(|z|^2)^{-1} \\ (\langle\widehat{\sin}(\phi)\rangle)^2 &= \sin^2\theta\, I_1(|z|)^2 \qquad \text{etc}\end{aligned} \tag{C2}$$

in terms of the universal $I_{1,2}(|z|)$ radial functions. In the PB case, the only difference is the absence of the $\frac{1}{4}e_q(|z|^2)^{-1}$ term which is negligible for $|z|^2$ large. Therefore, in the SG case, $Q(|z|,\theta) \to (4\cos\theta)^{-1}$ as $|z|^2 \to 0$ for all q.

In the region of macrodeformation, for $|z|^2$ sufficiently large in both the PB/SG cases by equations (43)–(53)

$$Q(|z|,\theta) \underset{q\to 0}{\longrightarrow} \begin{cases} (4\cos^2\theta)^{-1} & \text{at } |z_s|,\ s \geqslant 1 \\ \dfrac{2-\sin^2\theta}{4\cos^2\theta} & \text{at } |z_r|,\ r \geqslant 1 \end{cases} \tag{C3}$$

which agrees with figure 9.

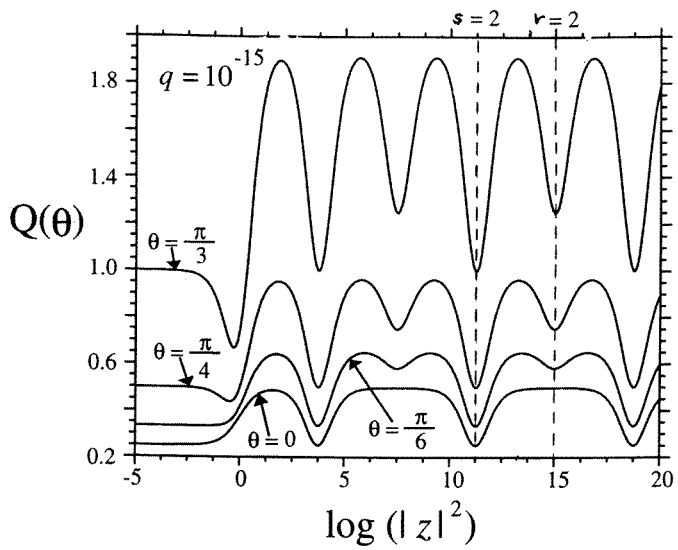

Figure 9. For $q = 10^{-15}$, behaviour of the minimization function $Q(|z|,\theta) \equiv (\Delta N)^2(\Delta\widehat{\sin}(\phi))^2/\langle\widehat{\cos}(\phi)\rangle^2 \geqslant \frac{1}{4}$ as a function of $|z|^2$ for various values of the phase θ. Only for $q = 1$ is $Q(|z|,\theta)$ minimized for $|z|^2 \geqslant 80$.

In figure 9 for $Q(|z|,\theta)$, as well as in figure 10 for $U(|z|)$, a maxima in these distributions against $\log(|z|^2)$ occurs before the dip at the step value $|z_s|^2 = [s + \frac{1}{2}]$ and another, of equal

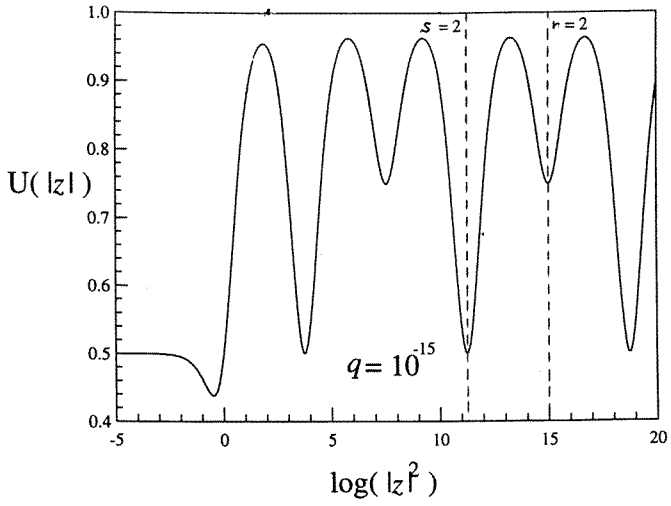

Figure 10. Behaviour of the Carruthers–Nieto minimization function $U(|z|) \geqslant \frac{1}{4}$, defined in equation (C12), as $\log(|z|^2)$ increases for fixed $q = 10^{-15}$. Only for $q = 1$ is $U(|z|)$ minimized for $|z|^2 \geqslant 80$.

height, occurs after it and before the mid-riser value $|z_r|^2 = [r + 1]$. In the $q \to 0$ limit, these positions correspond respectively to 'three-quarter' riser values of

$$|z_a|^2 = [a + \tfrac{1}{4}] \qquad a = 1, 2, \ldots$$
$$\approx \frac{q^{-\frac{1}{2}a+\frac{3}{8}}}{(1-q)} \tag{C4}$$

and to 'quarter' riser values of

$$|z_b|^2 = [b + \tfrac{3}{4}] \qquad b = 1, 2, \ldots$$
$$\approx \frac{q^{-\frac{1}{2}b+\frac{1}{8}}}{(1-q)}. \tag{C5}$$

Notice that these 'fractional' riser values are 'fractions' in the $\log_{10}|z|^2$ units of the horizontal axis in the figures. At $|z_a|^2 = [a + \frac{1}{4}]$, using the equation (17) approximation,

$$e_q(|z_a|^2) = \frac{[a+\frac{1}{4}]^a}{[a]!}\{1 + q^{1/8} + \cdots\} \tag{C6}$$

and

$$\langle N\rangle \to a - q^{1/8} + \cdots \qquad (\Delta N)^2 \to q^{1/8}$$
$$I_1 \to q^{1/16}(1 + \mathcal{O}(q^{3/8})) \qquad I_2 \to q^{1/4}(1 + q^{1/8}). \tag{C7}$$

Thus, at $|z_a|^2$ values, as $q \to 0$

$$Q \to \frac{1}{2\cos^2\theta} \qquad U \to 1 \qquad Q' \to \tfrac{1}{2}. \tag{C8}$$

Note that the 'three-quarter' riser value $|z_a|^2$, $\langle N\rangle$ lies below the ath step by only $q^{1/8}$ unlike for the mid-riser point at $|z_r|^2$ where $\langle N\rangle \to (r + \frac{1}{2})$ as per equation (25). Similarly, at the 'quarter' riser values, $\langle N\rangle$ lies above the bth step by $q^{1/8}$. So, indeed, the steps become flatter and longer as $q \to 0$.

At $|z_b|^2 = [b + \frac{3}{4}]$, it follows that

$$e_q(|z_b|^2) = \frac{[b+\frac{3}{4}]^b}{[b]!}\{1 + q^{1/8} + \cdots\} \tag{C9}$$

and

$$\begin{aligned} &\langle N\rangle \to b + q^{1/8} + \cdots \qquad (\Delta N)^2 \to q^{1/8} \\ &I_1 \to q^{1/16}(1 + \mathcal{O}(q^{3/8})) \qquad I_2 \to q^{1/4}(1 + q^{1/8}). \end{aligned} \tag{C10}$$

Thus, at $|z_b|^2$ the Q, U, and Q' limits as $q \to 0$ are also as in equation (C8). Notice in figures 9 and 10 that for finite $q = 10^{-15}$ the actual peak positions and peak values in Q and U corresponding to $|z_a|^2$ and $|z_b|^2$ are shifted from (C4), (C5) and (C9) towards the mid-riser values. For [11] the larger $q = 10^{-6}$, the shifting in the peak's value is almost complete in U.

C.2. $U(|z|)$

Similarly, since in the SG case

$$\langle\{\widehat{\cos}(\phi)\}^2\rangle = \tfrac{1}{2} + \tfrac{1}{2}\cos 2\theta\, I_2(|z|) - \tfrac{1}{4}e_q(|z|^2)^{-1} \tag{C11}$$

we find

$$\begin{aligned} U(|z|) &= (\Delta\hat{N})^2\left\{\frac{(\Delta\widehat{\sin}(\phi))^2 + (\Delta\widehat{\cos}(\phi))^2}{\langle\widehat{\sin}(\phi)\rangle^2 + \langle\widehat{\cos}(\phi)\rangle^2}\right\} \geqslant \frac{1}{4} \\ &= (\Delta\hat{N})^2\left\{\frac{1 - I_1(|z|) - \frac{1}{2}e_q(|z|^2)^{-1}}{I_1(|z|)^2}\right\} \end{aligned} \tag{C12}$$

with the $e_q(|z|^2)^{-1}$ terms in equations (C11) and (C12) again absent in the PB case. So again, $U(|z|) \to \frac{1}{2}$ as $|z|^2 \to 0$ for all q in the SG case. For $|z|$ sufficiently large, in both PB and SG cases, as $q \to 0$

$$U(|z|) \to \begin{cases} \frac{1}{2} & \text{at } |z_s|,\ s \geqslant 1 \\ \frac{3}{4} & \text{at } |z_r|,\ r \geqslant 1. \end{cases} \tag{C13}$$

C.3. $Q'(|z|, \theta)$

In the macrodeformed region the uncertainties in $\Delta\widehat{\sin}(\phi)$ and $\Delta\widehat{\cos}(\phi)$ are correlated for both the SG and PB phase operators. This can be seen by considering the function

$$Q'(|z|,\theta) \equiv \Delta\widehat{\sin}(\phi)\Delta\widehat{\cos}(\phi) \geqslant \tfrac{1}{4}e_q(|z|^2)^{-1}. \tag{C14}$$

In terms of $I_{1,2}(|z|)$

$$4\{Q'(|z|,\theta)\}^2 = \{1 - (I_1(|z|))^2 - \tfrac{1}{2}e_q(|z|^2)^{-1}\}^2 - \cos^2(2\theta)\{I_2(|z|) - (I_1(|z|))^2\}^2. \tag{C15}$$

In the PB case, the $e_q(|z|^2)^{-1}$ terms are absent in both expressions. So, in the SG case, $Q' \to \frac{1}{4}$ as $|z|^2 \to 0$ for all q. In the region of macrodeformation, for $|z|^2$ sufficiently large in both the PB/SG cases

$$Q'(|z|,\theta) \underset{q\to 0}{\longrightarrow} \begin{cases} \frac{1}{2} & \text{at } |z_s|,\ s \geqslant 1 \\ \frac{1}{8}(9 - \cos^2 2\theta)^{1/2} & \text{at } |z_r|,\ r \geqslant 1 \end{cases} \tag{C16}$$

which agrees with figure 11 for $q = 10^{-15}$. (At $q = 10^{-6}$, $Q'(|z_r|) \simeq 0.44$, and near the $|z_r|$ values the oscillations do not flatten out.)

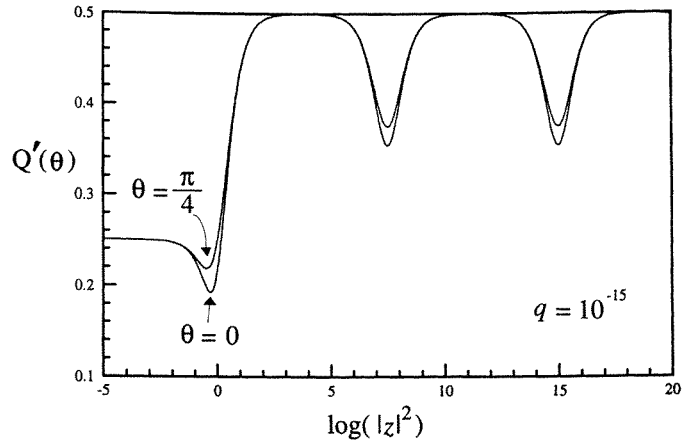

Figure 11. For $q = 10^{-15}$, behaviour of the product of the uncertainties of the q-analogue SG sine and cosine operators, $Q'(\theta) \equiv \Delta\widehat{\sin}(\phi)\Delta\widehat{\cos}(\phi)$. The associated SG operators, $\widehat{\sin}(\phi)$ and $\widehat{\cos}(\phi)$, are strongly correlated and non-classical in the $q < (\sim 10^{-6})$ region. In fact, only for $q = 1$ does $Q'(\theta)$ vanish for $|z|^2 \geqslant 80$.

This strong correlation in $\sin\hat{\phi}_q$ and $\cos\hat{\phi}_q$ for $q \neq 1$ is to be expected since for $|z|^2 \geqslant 80$ the PB phase distribution $\bar{P}_q(\theta_m)$ is no longer (approximately) a Dirac δ distribution, but instead $\bar{P}_q(\theta_m)$ has finite width.

Appendix D. Further properties of macrodeformed CSs

For an approximate state interpolating between $|z_s\rangle$ and $|z_r\rangle$ there is

$$|z_A\rangle = \mathrm{e}^{\mathrm{i}s\theta}\bar{N}_A\left\{|s\rangle + \frac{z}{[s+1]^{1/2}}|s+1\rangle\right\} \qquad \bar{N}_A = (1+|z|^2[s+1]^{-1})^{-1/2} \tag{D1}$$

with $\langle z_A|[N]|z_A\rangle = |z|^2$ and $a|z_A\rangle = z|z_A\rangle$. Note against the (mid)riser state, equation (19), in $|z_A\rangle$ the fixed superposition of $|s\rangle$ and $|s+1\rangle$ involves the modulus, $|z|$, and the phase θ of $z = |z|\mathrm{e}^{\mathrm{i}\theta}$. For instance, the approximate Fock states associated respectively with $|z_a\rangle$ and the quarter riser $|z_b\rangle$ of equations (C4) and (C5) are obtained by inserting z_a and z_b, into equation (D1). Fraction-in-$\langle N\rangle$ riser states can also be constructed with $|z|^2$ invariant under $q \leftrightarrow 1/q$: for example, with $L_{(\mathrm{even})}$ and $m_{(\mathrm{odd})} = 1, 3, \ldots, L-1$, define

$$|z_s^{L,m}|^2 \equiv \left(\frac{m}{L-m}\right)[s+1] \tag{D1a}$$

so by equation (D1)

$$|z_s^{L,m}\rangle \to \frac{1}{\sqrt{L}}\mathrm{e}^{\mathrm{i}s\theta}\left(\sqrt{L-m}|s\rangle + \mathrm{e}^{\mathrm{i}\theta}\sqrt{m}|s+1\rangle\right) \tag{D1b}$$

with

$$\langle N\rangle \to s + \frac{m}{L} \qquad (\Delta N)^2 \to \frac{m}{L}\left(1-\frac{m}{L}\right). \tag{D1c}$$

In terms of the PB phase state basis, see equation (42), approximate Fock-state forms for the step and riser states are respectively

$$|z_s\rangle \to \frac{1}{\sqrt{s'+1}}\sum_{m=0}^{s'}\mathrm{e}^{\mathrm{i}s(\theta-\theta_m)}|\theta_m\rangle \tag{D2}$$

$$|z_r\rangle \to \frac{1}{\sqrt{2(s'+1)}} \sum_{m=0}^{s'} \{e^{is\theta(\theta-\theta_m)} + e^{i(s+1)(\theta-\theta_m)}\}|\theta_m\rangle \tag{D3}$$

whereas

$$|z_A\rangle \to \frac{\bar{N}_A}{\sqrt{s'+1}} \sum_{m=0}^{s'} \left\{ e^{is(\theta-\theta_m)} + \frac{|z_A|}{[s+1]^{1/2}} e^{i(s+1)(\theta-\theta_m)} \right\} |\theta_m\rangle. \tag{D4}$$

The coefficients in these equations give the simple forms of the $\langle\theta_m|z_i\rangle$, $i = s, r, A$, amplitudes which occur as $q \to 0$.

The time evolution of $|z\rangle_q$ is the same as for the usual $q = 1$ CSs if the N-Hamiltonian $H_N \equiv \bar{h}\omega(N + \frac{1}{2})$ is responsible for the time evolution because

$$|z, t\rangle = \exp(-iH_N t/\bar{h})|z\rangle = \exp(-i\omega t/2)|z(t)\rangle$$

where $z(t) = |z| \exp\{i(\theta - \omega t)\}$. So ignoring the overall $\exp(-i\omega t/2)$ phase factor from the vacuum state energy, time evolution corresponds to the substitution $\theta \to (\theta - \omega t)$: for instance,

$$\langle z(t)|\hat{Q}|z(t)\rangle = (2\bar{h}/\omega)^{1/2}|z| \cos(\theta - \omega t)$$

and

$$\langle z(t)|\hat{P}|z(t)\rangle = (2\bar{h}\omega)^{1/2}|z| \sin(\theta - \omega t)$$

with time-independent variances

$$\frac{\omega}{\bar{h}}(\Delta\hat{Q})^2 = \frac{1}{\bar{h}\omega}(\Delta\hat{P})^2 = \lambda(|z|)$$

and minimum uncertainty

$$2\Delta Q \Delta P = |\langle[Q, P]\rangle| = i\bar{h}\lambda(|z|).$$

The time evolution of $|z_s\rangle$ is approximately that of the ordinary sth level elementary harmonic oscillator state and of $|z_r\rangle$ (and $|z_A\rangle$) is approximately that of the superposition of the two adjacent $|r\rangle$ and $|r+1\rangle$ levels (with time-independent probabilities to be in $|r\rangle$ and $|r+1\rangle$).

In contrast, the quadratic $\hat{P}, \hat{Q}$ Hamiltonian $H_{P,Q} \equiv \frac{1}{2}(\hat{P}^2 + \hat{Q}^2)$ does *not* possess conventional free-field properties with simple, orthodox physical interpretations, see the discussion in [4].

References

[1] MacFarlane A J 1989 *J. Phys. A: Math. Gen.* **22** 4581
Biedenharn L C 1989 *J. Phys. A: Math. Gen.* **22** L873

[2] Sun C P and Fu H C 1989 *J. Phys. A: Math. Gen.* **22** L983
Hayashi T 1990 *Commun. Math. Phys.* **127** 129
Chaichian M and Kulish P 1990 *Phys. Lett.* **234B** 72

[3] Damaskinski E V and Kulish P 1997 *Preprint* q-alg/961002, 9501006
Ueno K and Nishizawa M 1995 *Quantum Groups* ed J Lukierski (Warsaw: PWN)
Majid S 1995 *Foundations of Quantum Group Theory* (Cambridge: Cambridge University Press)
Biedenharn L C and Lohe M A 1995 *Quantum Group Symmetry and q-Tensor Algebras* (Singapore: World Scientific)
Chang Z 1995 *Phys. Rep.* **262** 137
Shnider S and Sternberg S 1993 *Quantum Groups* (Boston: International)
Zachos C 1992 *Contemp. Math.* **134** 351

[4] Nelson C A and Fields M H 1995 *Phys. Rev.* A **51** 2410
Chiu S-H, Gray R W and Nelson C A 1992 *Phys. Lett.* **164A** 237

Chung W-S 1996 *Gyeongsang Nat. Uni. Report* unpublished
[5] Nelson C A and Gartley M G 1994 *J. Phys. A: Math. Gen.* **27** 3857
Suny Bing 1996 On the two q-analogue logarithmic functions: $\ln_q(q), \ln\{e_q(z)\}$ *J. Phys. A: Math. Gen.* to appear
[6] Susskind L and Glogower J 1964 *Physics* **1** 49
[7] Pegg D T and Barnett S M 1988 *Europhys. Lett.* **6** 483
Pegg D T and Barnett S M 1989 *Phys. Rev.* A **39** 1665
[8] Lynch R 1995 *Phys. Rep.* **256** 367
Schleich W P and Barnett S M (eds) 1993 *Phys. Scr.* **T48** 3
[9] Fujikawa K 1995 *Phys. Rev.* A **52** 3299
Fujikawa K, Kwek L C and Oh C H 1995 *Mod. Phys. Lett.* A **10** 2543
[10] Carruthers P and Nieto M M 1965 *Phys. Rev. Lett.* **14** 387
Carruthers P and Nieto M M 1968 *Rev. Mod. Phys.* **40** 411
[11] Kimler W C IV 1996 *Thesis* State University of New York at Binghamton
[12] Prange R E and Girvin S M (eds) 1990 *The Quantum Hall Effect* (New York: Springer)
[13] Kimler W C IV and Nelson C A 1996 *Phys. Rev.* A **54** 3687
[14] Pegg D T and Barnett S M 1989 *J. Mod. Opt.* **36** 7
[15] Quesne C 1991 *Phys. Lett.* **153A** 303
Yu Z 1991 *J. Phys. A: Math. Gen.* **24** L1321
[16] Yu Z 1993 *Phys. Lett.* **175A** 391
[17] Klauder J R 1960 *Ann. Phys. NY* **11** 123
Rohrlich F 1970 *Analytic Methods in Mathematical Physics* ed R P Gilbert and R G Newton (New York: Gordon and Breach)